Charting ESCRT function reveals distinct and non-compensatory roles in blood progenitor maintenance and lineage choice in *Drosophila*

Arindam Ray, Yashashwinee Rai, Maneesha S Inamdar

Molecular Biology and Genetics Unit, Jawaharlal Nehru Centre for Advanced Scientific Research, Jakkur, Bangalore-560064, India

Abstract

Tissue heterogeneity permits diverse biological outputs in response to systemic signals but requires context-dependent spatiotemporal regulation of a limited number of signaling circuits. In addition to their stereotypical roles of transport and cargo sorting, endocytic networks provide rapid, adaptable, and often reversible means of signaling. Aberrant function of the Endosomal Sorting Complex Required for Transport (ESCRT) components results in ubiquitinated cargo accumulation, uncontrolled signaling and neoplastic transformation. However, context-specific effects of ESCRT on developmental decisions are not resolved. By a comprehensive spatiotemporal profiling of ESCRT in *Drosophila* hematopoiesis *in vivo*, here we show that pleiotropic ESCRT components have distinct effects on blood progenitor maintenance, lineage choice and response to immune challenge. Of all 13 core ESCRT components tested, only Vps28 and Vp36 were required in all progenitors, whereas others maintained spatiotemporally defined progenitor subsets. ESCRT depletion also sensitized posterior progenitors that normally resist differentiation, to respond to immunogenic cues. Depletion of the critical Notch signaling regulator Vps25 did not promote progenitor differentiation at steady state but made younger progenitors highly sensitive to wasp infestation, resulting in robust lamellocyte differentiation. We identify key heterotypic roles for ESCRT in controlling Notch activation and thereby progenitor proliferation and differentiation. Further, we show that ESCRT ability to regulate Notch activation depends on progenitor age and position along the anterior-posterior axis. The phenotypic range and disparity in signaling upon depletion of components provides insight into how ESCRT may tailor developmental diversity. These mechanisms for subtle control of cell phenotype may be applicable in multiple contexts.

Keywords

Blood cell homeostasis, Endosomal protein sorting, ESCRT, Progenitor homeostasis, Lineage choice, Ubiquitination, NICD, Notch signaling, Crystal Cell, Progenitor heterogeneity, Lamellocytes

33 **Significance**

34 The Endosomal Sorting Complex Required for Transport (ESCRT) machinery sorts ubiquitinated cargo
35 for degradation or recycling. Aberrant ESCRT function is associated with many blood disorders. We
36 did a comprehensive functional analysis of all 13 core ESCRT components in maintenance and
37 differentiation of *Drosophila* larval blood progenitors. We show that ESCRT have diverse and non-
38 compensatory functions in blood progenitors. ESCRT depletion from progenitors affects ubiquitination
39 status cell autonomously and independent of progenitor maintenance. ESCRT function is more critical
40 to maintain older progenitors and to prevent Notch-dependent crystal cell differentiation. Further,
41 ESCRT depletion sensitizes refractile younger progenitors for lamellocyte differentiation. Our *in situ*
42 developmental map of ESCRT function reveals critical checkpoints for cell fate choice and new
43 paradigms for generating progenitor heterogeneity.

Introduction

Tissue patterning requires spatiotemporally controlled cell proliferation, progenitor specification and lineage differentiation. While a limited number of signaling circuits impact these complex cell properties, their context-dependent regulation elicits multiple diverse biological outputs. Endocytic trafficking can maintain, attenuate or amplify signaling to regulate inter or intracellular communication [1]. In addition to their stereotypical roles of transport and cargo sorting, endocytic networks can regulate the behaviour of individual cells as well as groups or collectives, thereby significantly impacting tissue homeostasis.

Protein trafficking and turnover through the endolysosomal route allows rapid post-translational adjustment of signal transduction efficiency. The conserved Endosomal Sorting Complex Required for Transport (ESCRT) actively controls the sorting of ubiquitinated cargoes for lysosomal degradation. This hetero-multimeric complex consists of four subunits (ESCRT-0, I, II and III) that are sequentially recruited onto endomembrane-bound ubiquitinated cargoes, allowing them to be sequestered in the intraluminal vesicles (ILV) of the multivesicular bodies (MVB). The initial steps of recognition and binding of ubiquitinated cargoes, converge into the subsequent crucial steps of membrane remodelling during ILV formation. ESCRT components act in a co-operative manner, following defined molecular stoichiometry, to successfully sequester cargoes for degradation. Hence, phenotypic diversity of ESCRT mutants is rare in unicellular organisms like budding yeast. However, dysfunction of metazoan ESCRT components can manifest as distinct and diverse cellular and histological phenotypes such as defective MVB biogenesis and incorrect cell fate choice, tissue hyperproliferation, apoptotic resistance, etc due to aberrant activation of signaling pathways such as Notch, EGFR and JAK/STAT that alter tissue homeostasis[2-5].

Blood progenitors are exposed to a plethora of signals and need to respond to a rapidly changing environment for stem- and progenitor cell maintenance and controlled differentiation. Previous genetic screens and knockout-based functional analyses in both *Drosophila* and mouse models showed a role of ESCRT in maturation of specific blood cell types in erythroid and lymphoid lineages and a possible functional link of ESCRT to blood cell homeostasis [6-8]. Several key endosomal proteins such as Rabex5, Atg6, Rab5 and Rab11 actively control endocytic trafficking and are implicated in developmental signaling and blood cell homeostasis [9-13]. The blood cell-enriched conserved endosomal regulator of hematopoiesis, Asrij interacts with ADP Ribosylation Factor 1 (ARF1-GTP), regulates the endocytic proteome and maintains stemness of blood progenitors in the *Drosophila* lymph gland [14]. Loss of Asrij promotes activation of Notch signaling in hematopoiesis, thereby leading to precocious differentiation to crystal cells [14]. Also, *asrij* mutant hemocytes accumulate

77 Notch intracellular domain (NICD) in the sorting endosomes, mimicking an endosomal sorting defect.
78 Mouse Asrij also maintains hematopoietic stem cell quiescence [15]. This suggests conserved
79 mechanisms of endosomal protein sorting in blood cell homeostasis that merit further investigation.

80 The *Drosophila* larval lymph gland serves as a simple yet powerful model to study conserved
81 mechanisms of hematopoiesis *in situ*. Using this *in vivo* model, we investigated the role of ESCRT
82 components in spatiotemporal control of blood progenitor homeostasis and myelopoiesis. Blood
83 progenitors reside in the multi-lobed lymph gland that flanks the cardiac tube in segments T3 and A1.
84 The primary lobe of the lymph gland comprises of three distinct zones enriched in progenitors,
85 differentiated blood cells (plasmatocytes, crystal cells and lamellocytes) and the hematopoietic niche.
86 Blood progenitors of *Drosophila* are linearly arranged in anterior (primary) and posterior lobes
87 (secondary, tertiary and often quaternary) of the lymph gland and are characterized by the expression
88 of several markers such as Domeless, TepIV and DE-Cadherin. The lymph gland develops in an anterior
89 to posterior sequence, with younger progenitors in the posterior lobes [16]. Previous studies showed
90 that the progenitor population is heterogeneous in gene expression, mitochondrial morphology and
91 dynamics, signaling, differentiation potential and immune function [16, 17]. Posterior progenitors are
92 refractile to immune challenge due to immature mitochondrial morphology and differential activation
93 of JAK/STAT and Notch signaling [16, 17]. The lymph gland harbors the entire blood progenitor
94 population of *Drosophila*, and hence allows complete sampling and a comprehensive study of
95 progenitor homeostasis.

96 The *Drosophila* ESCRT is comprised of 13 core components [2, 18]. ESCRT-0 (Hrs, Stam) binds to the
97 ubiquitinated cargoes through a ubiquitin-interacting motif. It then recruits ESCRT-I (Vps28, Tsg101,
98 Vps37A, Vps37B) and ESCRT-II (Vps25, Vps22 and Vps36), which act as a bridging complex to assemble
99 ESCRT-III (Vps32, Vps24, Vps20, Vps2). ESCRT-I-dependent membrane inward budding (negative
100 curvature) and ESCRT-III-dependent membrane scission lie at the heart of endosomal protein sorting,
101 resulting in the formation of intraluminal vesicles (ILV) containing the sequestered cargo [19]. Vps32
102 is the principal filament-forming component that undergoes activation and polymerization upon
103 binding with various nucleating factors and integrates previous steps of endosomal sorting [5]. The
104 final step involves disassembly of ESCRT subunits and scission of the membrane neck of the
105 intraluminal vesicles, which is mediated by the Vps4-Vta1 mechanoenzyme complex.

106 Here, we provide a functional map of the role of all 13 *Drosophila* core ESCRT components in
107 ubiquitinated cargo sorting and blood cell lineage choice across distinct progenitor subsets. We show
108 that though ESCRT components are expressed in all cells of the lymph gland (LG), their roles in
109 controlling lineage-specific differentiation and immune response of blood progenitors are distinct and

110 position-dependent. We also find that ESCRT dysfunction primarily affects Notch activation-
111 dependent crystal cell differentiation. Our study supports heterogeneity of blood progenitors and
112 highlights the role of ESCRT in spatiotemporal segregation of signaling.

113

114

115 **Materials and methods**

116 **Fly stocks and genetics**

117 *Drosophila melanogaster* stocks were maintained at 25°C as described previously [14]. The details of
118 fly stocks, genetics and control genotypes used are in supplementary methods.

119

120 **Immunostaining analysis**

121 *Drosophila* third instar larval lymph glands were dissected in PBS as described before and
122 immunostained for microscopic analysis [20]. The detailed protocol and reagents used are in
123 supplementary methods.

124

125 **Wasp parasitism assay**

126 Wasp infestation was performed following standardised protocol as described in Rodrigues et al.,
127 2021a [16]. Details are mentioned in supplementary methods.

128

129 **Quantification and statistical analysis**

130 Blood cell differentiation was quantified as described in Ray et al., 2021 [17]. The details of
131 quantification of various parameters and statistical analysis are mentioned in supplementary
132 methods.

133

134

135

136 **Results**

137 **Divergent requirement for ESCRT components in ubiquitinated cargo sorting in the *Drosophila***
138 **lymph gland.**

139 To explore whether ESCRT function may determine blood progenitor identity or potential, we
140 depleted each of the 13 core ESCRT components individually in the lymph gland by RNAi mediated
141 knockdown (KD) in domeless (dome) expressing blood progenitors (*domeGal4>UAS ESCRT RNAi*). As
142 ESCRT plays an active role in ubiquitinated cargo sorting, the accumulation of ubiquitinated cargoes
143 serves as a hallmark of dysfunctional ESCRT machinery and impaired endosomal protein sorting. A
144 comprehensive analysis of conjugated ubiquitination (Ub) status (see methods) in the primary,
145 secondary and tertiary lobes by immunostaining the complete lymph gland showed a range of effects
146 with the phenotype varying among ESCRT components within a given ESCRT complex and between
147 complexes.

148 Control LG showed low or no Ub in primary, secondary, and tertiary lobes (Fig 1A, B). A similar trend
149 was seen on depletion of ESCRT-0 components Hrs or Stam, with an occasional increase in Ub in
150 primary lobes, which was not significant (Figure 1A, B). In contrast ESCRT-I, -II and -III depletion had
151 effects on all lobes, though not all components affected the Ub status. Among ESCRT-I components
152 (Vps28, Tsg101, Vps37A, Vps37B), depletion of Vps28 or Tsg101 very significantly increased Ub in the
153 primary lobe, Vps28 and Vps37A affected the secondary lobe and Vps37A showed an increase in Ub
154 in the tertiary lobe. Vps37B depletion had a mild non-significant effect on the Ub status of the LG
155 (Figure 1A, B). ESCRT-II components Vps25, Vps22 and Vps36 had no effect on the primary lobe.
156 However, Vps22 depletion caused a dramatic increase in Ub in the secondary and tertiary lobes, where
157 Vps25 and Vps36 depletion had no effect. Finally, depletion of ESCRT-III components (Vps32, Vps20
158 and Vps2) caused a significant increase in Ub in the primary lobes whereas secondary and tertiary
159 lobes were sensitive only to Vps20 depletion.

160 In summary, our data indicates non-uniform response of progenitors to perturbation of the cargo
161 sorting machinery, depending on the ESCRT component that is depleted as well as the target
162 progenitor population (Figure 1B schematic). Of the 13 core ESCRT components, 7 caused increased
163 Ub in the LG when depleted. Interestingly, the effects were not uniform amongst progenitor subsets
164 - 5 affected Ub status in the primary lobes, 4 in the secondary lobes and 3 in the tertiary lobes. This is
165 in agreement with the anterior-posterior developmental and functional heterogeneity of progenitors
166 reported earlier [16] and suggests that younger progenitors have a reduced requirement for ESCRT
167 function. Thus, our analysis provides a spatiotemporal correlation of Ub status to ESCRT depletion in

168 LG progenitor subsets. We next tested whether this correlation reflects the response of progenitors
169 to maintenance and differentiation cues.

170

171 **ESCRT components play distinct roles in lymph gland progenitor maintenance.**

172 As ESCRT components regulate ubiquitinated cargo sorting in the blood progenitors, they might
173 potentially regulate progenitor homeostasis. Hence, we checked whether depleting the 13 ESCRT
174 components individually from dome^{+} progenitor subsets (marked by GFP expression)
175 (*domeGal4>2XEGFP/+; UAS ESCRT-RNAi/+; +/+*) may affect progenitor status similar to the effect on
176 Ub accumulation. As in the case of Ub status, a comprehensive analysis of progenitor fraction (see
177 methods) in the primary, secondary, and tertiary lobes of the lymph gland showed a range of effects
178 with the phenotype varying among ESCRT components within a complex and between complexes
179 (Figure 2A, B). Assessment of mitotically active nuclei and cell counts showed that ESCRT affects
180 proliferation of blood progenitors (Fig S1A-C; see supplementary results).

181 In controls, anterior lymph gland lobe progenitors are restricted to the inner medullary zone (MZ)
182 while the posterior lobes are composed almost entirely of progenitors [16]. ESCRT-0 (Hrs, Stam)
183 knockdown did not show any significant change in progenitor status indicating non-essential roles for
184 these in progenitor maintenance (Fig 2A, B). Depletion of ESCRT-I components Vps28 and Tsg101
185 caused reduction in progenitor fraction in the primary lobes whereas secondary lobe progenitors were
186 reduced by depletion of Vps28, Vps37A or Vps37B but not of Tsg101. Interestingly, ESCRT-I
187 components had no effect on tertiary lobe progenitors. Among ESCRT-II components, Vps25 had an
188 effect on proliferation causing an absolute increase in primary lobe cell numbers with a concomitant
189 decrease in progenitor fraction (Fig 2A, B; S1A, C; S6; Supplementary results). Vps22 also did not affect
190 LG progenitor fraction. In contrast, Vps36 drastically reduced progenitor fraction in all LG lobes, with
191 phenotype severity increasing from anterior to posterior. ESCRT-III had very restricted effects on
192 progenitors with Vps32 KD causing a reduction only in anterior progenitors, Vps2 KD reduced both
193 anterior and posterior progenitors and Vps24 and Vps20 had no effect (Fig. 2A-C).

194 Since increased Ub accumulation indicates dysfunctional cargo sorting and this is likely a cause of
195 progenitor loss, we compared Ub status on ESCRT KD with progenitor maintenance. Superimposition
196 of the phenotype chart for each of these (Fig 6B, C) showed that there was no absolute correlation
197 between increased Ub and reduced progenitor numbers in older (primary lobe) or younger (posterior
198 lobes) progenitors. While knockdown of some ESCRT components [(Vps28, Tsg101 (ESCRT-I), Vps32
199 and Vps2 (ESCRT-III)] caused increased Ub and reduced progenitors in the primary lobe, others

200 [(Vps25, Vps36 (ESCRT-II)] showed no change in Ub but progenitor numbers were reduced. Similarly,
201 knockdown of Vps20 (ESCRT-III) had increased Ub but no effect on progenitors. Hence in addition to
202 Ub cargo sorting, ESCRT components Vps25 and Vps36 have a critical independent role in progenitor
203 maintenance. Notably, there was no correlation at all between Ub increase and progenitor reduction
204 in the youngest progenitors (tertiary lobe). This suggests that notwithstanding defects in cargo sorting,
205 posterior progenitors remain less sensitive to perturbation, indicating that they are maintained by
206 other robust mechanisms.
207

208 **Older progenitors are more prone to plasmatocyte differentiation upon ESCRT depletion**

209 Plasmatocytes, marked by P1 expression, make up about 95% of the differentiated hemocyte
210 population. In the LG, they are restricted to the cortical zone of the primary lobe, with occasional P1
211 positive cells seen in posterior lobes. Reduced progenitor numbers are expected to be accompanied
212 by an increase in the plasmatocyte population due to differentiation. Enumeration of P1 positive cells
213 in the ESCRT KD LG (*domeGal4 UAS 2XEGFP> UAS ESCRT RNAi*) showed an expected increase in the
214 plasmatocyte fraction of the primary lobe for Vps28, Tsg101, Vps36 and Vps32, where the progenitor
215 fraction was mostly reduced (Fig 2A, C) However, Vps25 depletion had no apparent effect on
216 differentiation. This could be due to the failure of progenitors to terminally differentiate into
217 plasmatocytes or due to non-autonomous overproliferation of the intermediate population.
218 Additionally, Vps22 KD also showed increased plasmatocyte numbers though there was no significant
219 effect on the progenitor fraction, suggesting possible non-autonomous overproliferation or
220 exhaustion of the intermediate population. The remaining ESCRT components had no effect on
221 primary lobe plasmatocytes. Interestingly, KD of ESCRT-0 component Hrs and ESCRT-III component
222 Vps32, that had no effect on progenitors, caused an increase in plasmatocyte numbers only in the
223 secondary lobes. This indicates that though there is no effect as assessed by progenitor marker
224 analysis, Hrs or Vps32 depletion has sensitized the tissue to respond to proliferation and
225 differentiation cues. Along similar lines, Vps36 and Vps2 depletion drastically reduced the secondary
226 progenitor fraction and increased plasmatocyte differentiation. Except for Vps28, ESCRT KD did not
227 induce plasmatocytes in the tertiary lobes, even when progenitors were lost (e.g. Vps36 KD and Vps2
228 KD).

229

230

231 **ESCRT components are most effective in suppressing the crystal cell lineage.**

232 Crystal cells make up only about 5% of the differentiated hemocyte pool. Under steady state
233 conditions each primary lobe harbors approximately 0-10 crystal cells, while they are generally absent
234 from posterior lobes, even upon immune challenge [16]. As seen earlier, 8 of the 13 core ESCRT
235 components affect progenitor numbers in one or more lobes (Fig 3A, B). Further these effects are
236 position-dependent. Hence, we next analysed crystal cell status by checking expression of ProPO in
237 the ESCRT depleted LGs.

238 Knockdown of 12 out of 13 ESCRTs increased crystal cell differentiation in the primary lobes. Vps25
239 depletion in the progenitors had no effect on crystal cell differentiation. Secondary lobes were
240 sensitive to depletion of Hrs, Vps28, Vps36 and Vps2 showing increased crystal cell numbers in all
241 cases. Tertiary lobes showed increase in crystal cell numbers only on Vps28 or Vps36 depletion. This
242 suggested that cargo sorting is critical to regulate crystal cell differentiation. Perturbation in the ESCRT
243 machinery results in activation of signaling pathways that promote crystal cells. Since Notch pathway
244 activation is a key requirement of crystal cell differentiation and Notch is a well-known target of
245 ESCRT-mediated cargo sorting [3, 21-23], we next checked for the status of Notch pathway activation
246 upon ESCRT depletion.

247

248 **ESCRT depletion in blood progenitors ectopically activates Notch signaling.**

249 Increased crystal cell differentiation upon depletion of some ESCRT components suggests that they
250 normally suppress Notch pathway activation. We focused our study on analysis of 8 ESCRT
251 components [Hrs, Stam (ESCRT-0); Vps28, Tsg101 (ESCRT-I); Vps25, Vps22 (ESCRT-II); Vps32, Vps24
252 (ESCRT-III)] as these are well known for their role in NICD trafficking and Notch pathway activation [2,
253 4]. These components showed uniform expression across different lobes and developmental zones of
254 the lymph gland, as assessed by immunofluorescence (IF) or RNA *in situ* hybridisation in wild type
255 lymph gland (Fig S2). *DomeGal4* driven knockdown of the ESCRT components was validated using
256 immunofluorescence analysis where antibodies were available or by *in situ* hybridisation and RT-qPCR
257 for analysing transcript levels (Fig S3). The Notch response element driving GFP (NRE-GFP) is a useful
258 reporter to assess activation of Notch signaling. Upon KD in the lymph gland progenitors, except
259 Vps25, all components tested [Hrs, Stam (ESCRT-0); Vps28, Tsg101 (ESCRT-I); Vps22 (ESCRT-II); Vps32,
260 Vps24 (ESCRT-III)] caused upregulation of Notch signaling as interpreted by an increase in NRE-GFP
261 positive cells in the primary lobe (Fig 4A). This is in concordance with the crystal cell differentiation
262 phenotype as all of the ESCRT components except Vps25 cause increased crystal cell differentiation in

263 the primary lobe upon knockdown. Our result also indicates that these 7 ESCRT components are
264 indispensable for regulation of Notch signaling in the blood cell progenitors possibly with non-
265 compensatory roles.

266 Knockdown of 3 out of the 8 ESCRT components [Hrs, Stam (ESCRT-0) and Vps28 (ESCRT-I)] resulted
267 in increased Notch signaling activation in the secondary lobe (Fig 4A, S4A). Of these only Hrs and Vps28
268 knockdown resulted in increased crystal cell differentiation in the secondary lobe (Fig 3), suggesting
269 additional mechanisms downstream of Notch activation prevent crystal cell differentiation in the
270 absence of Stam. Interestingly, in the tertiary lobe, both Hrs or Stam knockdown resulted in Notch
271 activation (Fig4A, S4A) though neither resulted in crystal cell differentiation (Fig 3). In either case,
272 tertiary lobe progenitors fail to differentiate, indicating their immature nature (Fig4A, S4A). Also,
273 though Vps28 depletion does not significantly activate Notch signaling in the tertiary lobe it can
274 promote crystal cell differentiation, suggesting a possible mechanism to downregulate Notch signaling
275 likely after progenitors differentiate. However, we do see occasional increase in Notch activation in
276 Vps28 KD tertiary lobes. Hence, crystal cell differentiation in the tertiary lobe could be under complex
277 temporal regulation. Our analysis demonstrates the active role of ESCRT components in regulating
278 Notch signaling, which may contribute to crystal cell differentiation and also differential response of
279 the progenitor subsets.

280 NICD cleavage and transport to the nucleus to activate target gene transcription is key to effecting
281 canonical and non-canonical modes of Notch signaling. Accumulation of NICD may lead to aberrant
282 activation of Notch signaling. Progenitor-specific knockdown of all tested ESCRT components, except
283 Vps25, resulted in increase in the number of cells accumulating NICD in the primary lobe (Fig 4B). This
284 suggests a role for a majority of the ESCRT components in NICD trafficking, which may affect Notch
285 signaling. The absence of any phenotype due to Vps25 knockdown suggests compensatory
286 mechanisms may regulate cargo trafficking and lineage-specific signaling activation, which is sufficient
287 to maintain progenitors at steady state.

288 Knockdown of 4 components [Hrs, Stam (ESCRT-0), Vps28 (ESCRT-I) and Vps24 (ESCRT-III)] led to an
289 increase in the number of NICD accumulating cells in the secondary lobe (Fig 4B, S4A). However, only
290 Hrs and Stam knockdown resulted in NICD accumulation in the tertiary lobe. This is in concordance
291 with the phenotype of Notch activation upon Hrs, Stam and Vps28 knockdown in the posterior lobes.
292 Our results show that NICD accumulation and Notch pathway activation correlate perfectly with
293 crystal cell differentiation upon ESCRT knockdown. Notch signaling is known to be sensitive to
294 endocytic sorting defects due to ESCRT in other contexts [24]. Similar effects may result in ectopic
295 activation and promoting crystal cell differentiation. Despite a differential effect on NICD trafficking

296 and Notch activation across progenitor subsets, immunolocalization and proximity ligation assay
297 indicated uniform interaction of ESCRT with NICD (Fig S4B, C; see supplementary results). Also, Notch
298 activation triggered by ESCRT depletion in blood progenitors may be independent of the status of
299 Notch ubiquitination (Fig S4D, E; see supplementary results). Hence the role of ESCRT in Notch
300 signaling may lie downstream of subtle post-translational regulatory mechanisms.

301

302 **ESCRT depletion sensitizes progenitors for lamellocyte differentiation.**

303 Lamellocytes are rarely present in the larva without any wasp infestation. However, progenitor-
304 specific knockdown of 6 ESCRT components [Tsg101 and Vps37A (ESCRT-I); Vps36 (ESCRT-II); Vps32,
305 Vps20 and Vps2 (ESCRT-III)] induced lamellocyte differentiation in the primary lobe, as visualized by
306 Phalloidin (F-actin) staining, even without any immune challenge (Fig 5A-C). Only 2 components
307 (Vps36 and Vps2) caused lamellocyte differentiation in the secondary lobe when knocked down and
308 only Vps36 knockdown triggered lamellocyte differentiation in the tertiary lobe (Fig 5A, B). This
309 indicates that the majority of the ESCRT components are not involved in suppressing lamellocyte
310 differentiation in the refractile posterior progenitors at steady state. However, it is likely that KD
311 progenitors may be more sensitive to immunogenic cues as compared to normal, unperturbed
312 progenitors.

313 Wild type larvae are generally able to mount a sufficiently robust immune response against wasp
314 infestation, that aids their survival and eclosion. Systemic signals are generated upon wasp infestation
315 and are received by the lymph gland progenitors [25], possibly through a complex extracellular matrix
316 [16]. This results in lamellocyte differentiation in the primary lobe followed by disintegration and
317 release of lamellocytes into circulation. Secondary and tertiary lobes are refractile to wasp infestation
318 and do not form lamellocytes even upon immune challenge. Hence, we chose to test the response to
319 wasp infestation in- a] ESCRT KD that had no effect on lamellocyte formation (Vps25 KD) and b] ESCRT
320 KD that caused lamellocyte differentiation only in the primary lobe (Vps32 KD). Knockdown of both
321 Vps25 and Vps32 triggered lamellocyte differentiation across all progenitor subsets upon immune
322 challenge with wasp (Fig 5C). This shows that Vps25 and Vps32 play essential roles in preventing all
323 posterior progenitors from lamellocyte differentiation in response to a natural immune challenge.
324 Further, loss of ESCRT sensitizes progenitors to systemic cues by unlocking differentiation programs.

325 Our detailed analyses of blood progenitor differentiation upon knockdown of the 13 core ESCRT
326 components yielded a functional map that reflects distinct lineage-specific roles of ESCRT in blood cell
327 homeostasis and reduced sensitivity of younger progenitors to endocytic perturbation (Fig 6 A, B).

328 **ESCRT regulates cargo sorting in a cell-autonomous manner in blood progenitors.**

329 Progenitor-specific downregulation of ESCRT expression leads to accumulation of ubiquitinated
330 cargoes. However, a majority of the ubiquitin aggregates were found to accumulate in non-progenitor
331 (domeless^{-}) cells, suggesting a possible cell non-autonomous effect. To test whether this could be due
332 to ubiquitin accumulation in progenitors prior to their differentiation (cells lose domeless marker
333 expression), we generated homozygous mutant mitotic recombinant clones for a representative
334 ESCRT gene Vps32 (shrub), in progenitors. Vps32 is a terminally acting ESCRT that affects ubiquitinated
335 cargo sorting and its depletion affects all blood cell lineages (Fig. 6). Hence it serves as a good model
336 to assess cell autonomous function of ESCRT. Staining for conjugated ubiquitin revealed accumulation
337 of ubiquitin aggregates in the homozygous mutant patch of the tissue (GFP^{-}) indicating Vps32 has a
338 cell autonomous role in cargo sorting in blood progenitors (Fig 7A). Hence, it is likely that ubiquitin
339 seen in dome^{-} cells (Fig. 1) accumulated when the cells were still expressing domeless. This suggests
340 that despite a decrease in dome expression in the knockdown cells, ubiquitin aggregates may persist
341 during differentiation, likely due to dysfunctional cargo sorting in a cell-autonomous manner.

342

343 **ESCRT affects progenitor differentiation in a cell non-autonomous manner.**

344 We analysed differentiation in progenitor-specific mitotic clones of ESCRT. Vps32 knockdown results
345 in increased crystal cell differentiation and triggers lamellocyte differentiation, as described earlier
346 (Fig 3, 5-6). ProPO staining showed both wild type and mutant origin of crystal cells as revealed by
347 overlap with GFP expression in the mutant tissue (Fig 7B). As crystal cells are usually present in the
348 lymph gland in low numbers, it is difficult to interpret cell-autonomous origin of crystal cells from
349 mutant progenitors. However, lamellocytes are completely absent in the control lymph gland at
350 steady state (Fig 7C). Phalloidin staining in the Vps32 mutant clone showed GFP^{+} elongated or
351 coalescing cells, indicating the presence of lamellocytes and possibly their precursors (Fig 7C). This
352 suggests non-autonomous regulation of lamellocyte differentiation by ESCRT. Hence, ESCRT may
353 regulate progenitor differentiation in both a cell-autonomous as well as non-cell-autonomous
354 manner.

355 Vps25 knockdown did not affect the status of ubiquitination, progenitor maintenance or
356 differentiation to any particular blood cell lineage despite its expression in the lymph gland. To further
357 verify this, we generated lymph gland progenitor-specific homozygous mitotic clones of Vps25 loss of
358 function mutation (Vps25^{A3}). There was no accumulation of ubiquitin aggregates (Fig S5A) or any
359 change in the status of the progenitor (Fig S5B), plasmatocyte (Fig S5C), crystal cell (Fig S5D) and

360 lamellocyte differentiation (Fig S5E). However, the mutant lymph glands showed enlargement of the
361 primary lobe, suggesting possible increase in blood cell proliferation upon loss of Vps25, due to non-
362 autonomous effects. Also, phalloidin staining revealed appearance of binucleate, large cells and also
363 very small cells occasionally, along with increase in F-actin content in some patches of the tissue,
364 mostly in a cell autonomous manner (visible in GFP negative area of the tissue) (Fig S5E). Hence, Vps25
365 possibly inhibits uncontrolled cell proliferation and may contribute to critical steps of cell division that
366 may dictate cell shape, number and polarity.

367

368

369 **Discussion**

370 Cargo sorting by the ESCRT machinery is a ubiquitous requirement. We asked whether ESCRTs play a
371 decisive role in progenitor maintenance and lineage choice during development. For this we chose the
372 well-conserved *Drosophila* hematopoietic system as a model. It is a simple, accessible and genetically
373 tractable developmental model with limited cell types, whose development is regulated by conserved
374 signaling networks.

375 Our study shows the active role of endosomal protein sorting in hematopoietic homeostasis *in vivo*.
376 The detailed functional map of all 13 ESCRT core components in lymph gland hematopoiesis highlights
377 distinct regulatory roles of individual components in lineage-specific progenitor differentiation. The
378 functional chart reveals the most crucial steps of endosomal protein sorting in blood progenitor fate
379 choice. ESCRT-I remodels the endosomal membrane through budding and ESCRT-III carries out
380 scission, to allow cargo sorting. Loss of ESCRT-I or ESCRT-III components result in progenitor
381 differentiation to all blood cell lineages. Moreover, Vps28 knockdown significantly affects crystal cell
382 differentiation in all lymph gland lobes and Vps2 depletion induces posterior progenitor
383 differentiation to lamellocytes. Hence, membrane budding and scission during endosomal protein
384 sorting appear to affect a wide range of signaling pathways across distinct progenitor subsets. Recent
385 reports highlight the universal role of ESCRT-III, often in concert with ESCRT-I, in various ESCRT-
386 dependent membrane remodelling processes such as nuclear envelope reformation, lysosomal
387 membrane repair, cytokinetic abscission, macroautophagy and exocytosis [5]. Whether such
388 moonlighting functions of ESCRT-I and ESCRT-III impact signaling that determines lineage specification
389 merits further investigation.

390 Curiously, we observed drastic functional diversity of ESCRT-II components in progenitor fate
391 specification. While Vps36 depletion affected all lineages across progenitor subsets, Vps25 depletion

392 did not affect differentiation. Loss of Vps25 caused hyperproliferation in blood cells and failed to
393 activate signaling pathways such as Notch, which are necessary for progenitor differentiation. Though
394 Vps25 is a critical player in endosomal protein sorting in epithelial tissues [23, 26], its redundancy in
395 lineage-specific differentiation suggests alternate routes for endosomal protein sorting in blood
396 progenitors or a temporally regulated, developmental stage-specific role that has not yet been
397 identified. Notably, though Vps25 is dispensable for steady state hematopoiesis, its depletion
398 sensitizes all progenitors to differentiate upon immune challenge. This supports the possibility that
399 the diverse roles of ESCRT may contribute to differential regulation of steady state and stress
400 hematopoiesis.

401 Our study shows the distinct role of individual components of ESCRT in Notch signaling in blood
402 progenitors. Expectedly, regulation of Notch signaling in lymph gland progenitors relies heavily on the
403 ESCRT machinery. Our previous reports highlight the potential functional link of endosomal protein
404 sorting with blood progenitor homeostasis [14, 27]. Though Hrs and Stam depletion promoted crystal
405 cell differentiation in the lymph gland, it hardly affected plasmatocyte and lamellocyte differentiation.
406 In epithelial tissue, though Hrs and Stam regulate Notch trafficking, they do not regulate Notch
407 pathway activation and downstream phenotypes such as cell polarity and proliferation [4]. Similar
408 mechanisms specific to hematopoietic tissue are not yet explored. It is notable that ALIX and its yeast
409 homolog Bro1 can recognize non-ubiquitinated cargoes and sort them independent of ESCRT-0 [28].
410 Also, Bro1, ALIX and HD-PTP act as alternate bridging factors to ESCRT-II to mediate endosomal protein
411 sorting in yeast and mammalian cells [29, 30]. Even post-translational regulatory mechanisms may
412 render ESCRT components inactive [31]. The non-compensatory roles of only a limited number of
413 ESCRT components, in spite of uniform expression across the lymph gland, supports the idea that
414 endosomal protein sorting possibly acts through multiple analogous components and parallel routes,
415 with only a few indispensable, critical regulatory nodes.

416 ESCRT may potentially regulate EGFR cargo transport, sorting and signaling activation that governs
417 plasmatocyte proliferation and lamellocyte differentiation. Also, JAK/STAT and Hedgehog signaling
418 can be regulated at the level of endosomal sorting in the blood progenitor. We speculate that lineage-
419 specific signaling activation could be achieved through modulation of individual ESCRT component
420 expression and function at the post-transcriptional or post-translational level. Though Deltex and
421 eIF3f1 positively regulate Notch signaling in epithelial tissues [32-34], they appear dispensable for
422 controlling Notch activation in blood progenitors upon ESCRT knockdown. While other E3 ubiquitin
423 ligases and deubiquitinases may possibly complement for Deltex or eIF3f1 depletion, signaling
424 activation may not always depend on the status of ubiquitination. For example, Vps36 depletion elicits
425 a strong phenotype of differentiation without causing ubiquitinated cargo accumulation. Further

426 genetic interaction-based studies with other regulators of Notch signaling may reveal ESCRT-
427 dependent mechanisms of Notch activation.

428 Lymph gland progenitor subsets are functionally heterogeneous and show reduced sensitivity to
429 differentiation cues from anterior to posterior [16, 17]. Posterior progenitors resist differentiation
430 upon immune challenge suggesting that they have additional signal regulatory checkpoints. What
431 remains largely underexplored is the mechanism through which progenitor subsets differentially
432 respond to systemic cues. One possibility is that younger progenitors have inherently low levels of
433 ubiquitination and protein turnover and hence show mild effects on ESCRT depletion. Depletion of
434 Vps36 and Vps2 can trigger lamellocyte differentiation in refractile progenitors even without any
435 immune challenge, indicating that they actively prevent differentiation. Also, while Hrs knockdown
436 activates Notch signaling and crystal cell differentiation in posterior progenitors, Stam knockdown fails
437 to trigger terminal differentiation to crystal cells despite Notch activation. This indicates existence of
438 multiple checkpoints and highlights the complexity of mechanisms that progenitors may employ to
439 maintain their identity. Elucidating expression and function at the single cell level may aid in an
440 improved understanding of ESCRT-dependent lineage specification across these distinct progenitor
441 subsets. Such candidates can be screened further for efficient modulation of vertebrate blood
442 regeneration *in vitro* as well as *in vivo*.

443 Loss of function mutation in ESCRT genes result in cell-autonomous cargo accumulation in *Drosophila*
444 epithelial tissues [2, 3]. However, the cell non-autonomous role of ESCRT in cell proliferation as well
445 as neoplastic transformation, suggests altered intercellular communication and aberrant signaling
446 activation in the neighboring cell population [2, 3, 23]. In concordance with the previous reports, we
447 observed a cell-autonomous role of ESCRT in regulating ubiquitinated cargo sorting in the blood
448 progenitors. However, analysis of lamellocyte differentiation suggests that ESCRT may regulate
449 lineage-specification non-autonomously. Both progenitor differentiation and proliferation can
450 influence blood cell homeostasis in the lymph gland. ESCRT depletion not only activates lineage-
451 specific signaling pathways but also promotes blood cell proliferation. Cell type-specific increase in
452 proliferation and enlargement of lymph gland lobes can affect the proportion of different types of
453 hemocytes. Elucidating the interplay between ESCRT components and the mitogenic signaling
454 machinery could reveal whether downregulation of mitotic potential may restore steady state
455 hematopoiesis.

456 BloodSpot Leukemia MILE and COSMIC databases show aberrant expression of ESCRT genes in
457 hematopoietic and lymphoid tissues in acute lymphoblastic leukemia (ALL), acute myeloid leukemia
458 (AML), myelodysplastic syndromes, etc (https://servers.binf.ku.dk/bloodspot/;

459 https://cancer.sanger.ac.uk/cosmic). Our study has application in understanding endosomal
460 regulation of proliferative hematological pathologies. Further, as the role of endosomal protein
461 sorting and the ESCRT machinery in vertebrate hematopoiesis is largely unexplored, it could help
462 identify new regulators of hematopoietic homeostasis and provide novel targets for therapies,
463 especially for improved blood regeneration during autologous transplantation. Further understanding
464 of context-specific functions of ESCRT may improve our understanding of lineage-specific regeneration
465 of tissue, including blood.

466

467

468 **Acknowledgements**

469 This work was funded by grants to M.S.I from SERB and JC Bose fellowship, Department of Science and
470 Technology, Government of India, LSRET grant from Department of Biotechnology and Jawaharlal
471 Nehru Centre for Advanced Scientific Research (JNCASR), Bangalore. We thank JNCASR confocal
472 facility for access and our laboratory members for helpful discussions.

473

474

475 **Author Contributions**

476 A.R. and M.S.I. designed research; A.R. and Y.R. performed experiments; M.S.I. contributed reagents
477 and materials; A.R., Y.R. and M.S.I. analysed the data; AR and MSI wrote the manuscript.

478

479

480 **Competing interest**

481 The authors declare no competing interest.

482

483

484

485 **References**

486 1. Di Fiore, P.P., and von Zastrow, M. (2014). Endocytosis, signaling, and beyond. Cold Spring
487 Harb Perspect Biol *6*.
488 2. Vaccari, T., Rusten, T.E., Menut, L., Nezis, I.P., Brech, A., Stenmark, H., and Bilder, D. (2009).
489 Comparative analysis of ESCRT-I, ESCRT-II and ESCRT-III function in Drosophila by efficient
490 isolation of ESCRT mutants. Journal of Cell Science *122*, 2413-2423.
491 3. Herz, H.M., Woodfield, S.E., Chen, Z., Bolduc, C., and Bergmann, A. (2009). Common and
492 distinct genetic properties of ESCRT-II components in Drosophila. PLoS One *4*, e4165.
493 4. Tognon, E., Wollscheid, N., Cortese, K., Tacchetti, C., and Vaccari, T. (2014). ESCRT-0 is not
494 required for ectopic Notch activation and tumor suppression in Drosophila. PLoS One *9*,
495 e93987.
496 5. Vietri, M., Radulovic, M., and Stenmark, H. (2019). The many functions of ESCRTs. Nat Rev Mol
497 Cell Biol.
498 6. Avet-Rochex, A., Boyer, K., Polesello, C., Gobert, V., Osman, D., Roch, F., Auge, B., Zanet, J.,
499 Haenlin, M., and Waltzer, L. (2010). An in vivo RNA interference screen identifies gene
500 networks controlling Drosophila melanogaster blood cell homeostasis. BMC Dev Biol *10*, 65.
501 7. Adoro, S., Park, K.H., Bettigole, S.E., Lis, R., Shin, H.R., Seo, H., Kim, J.H., Knobeloch, K.P., Shim,
502 J.H., and Glimcher, L.H. (2017). Post-translational control of T cell development by the ESCRT
503 protein CHMP5. Nat Immunol *18*, 780-790.
504 8. Liu, Y., Mei, Y., Han, X., Korobova, F.V., Prado, M.A., Yang, J., Peng, Z., Paulo, J.A., Gygi, S.P.,
505 Finley, D., et al. (2021). Membrane skeleton modulates erythroid proteome remodeling and
506 organelle clearance. Blood *137*, 398-409.
507 9. Shravage, B.V., Hill, J.H., Powers, C.M., Wu, L., and Baehrecke, E.H. (2013). Atg6 is required for
508 multiple vesicle trafficking pathways and hematopoiesis in Drosophila. Development *140*,
509 1321-1329.
510 10. Xia, P., Wang, S., Huang, G., Zhu, P., Li, M., Ye, B., Du, Y., and Fan, Z. (2014). WASH is required
511 for the differentiation commitment of hematopoietic stem cells in a c-Myc-dependent
512 manner. J Exp Med *211*, 2119-2134.
513 11. Reimels, T.A., and Pfleger, C.M. (2015). Drosophila Rabex-5 restricts Notch activity in
514 hematopoietic cells and maintains hematopoietic homeostasis. J Cell Sci *128*, 4512-4525.
515 12. Yu, S., Luo, F., and Jin, L.H. (2021). Rab5 and Rab11 maintain hematopoietic homeostasis by
516 restricting multiple signaling pathways in Drosophila. Elife *10*.
517 13. Evans, C.J., Olson, J.M., Mondal, B.C., Kandimalla, P., Abbasi, A., Abdusamad, M.M., Acosta,
518 O., Ainsworth, J.A., Akram, H.M., Albert, R.B., et al. (2021). A functional genomics screen
519 identifying blood cell development genes in Drosophila by undergraduates participating in a
520 course-based research experience. G3 (Bethesda) *11*.
521 14. Kulkarni, V., Khadilkar, R.J., Magadi, S.S., and Inamdar, M.S. (2011). Asrij maintains the stem
522 cell niche and controls differentiation during Drosophila lymph gland hematopoiesis. PLoS
523 One *6*, e27667.
524 15. Sinha, S., Dwivedi, T.R., Yengkhom, R., Bheemsetty, V.A., Abe, T., Kiyonari, H., VijayRaghavan,
525 K., and Inamdar, M.S. (2019). Asrij/OCIAD1 suppresses CSN5-mediated p53 degradation and
526 maintains mouse hematopoietic stem cell quiescence. Blood *133*, 2385-2400.
527 16. Rodrigues, D., Renaud, Y., VijayRaghavan, K., Waltzer, L., and Inamdar, M.S. (2021).
528 Differential activation of JAK-STAT signaling reveals functional compartmentalization in
529 Drosophila blood progenitors. Elife *10*.
530 17. Ray, A., Kamat, K., and Inamdar, M.S. (2021). A Conserved Role for Asrij/OCIAD1 in Progenitor
531 Differentiation and Lineage Specification Through Functional Interaction With the Regulators
532 of Mitochondrial Dynamics. Front Cell Dev Biol *9*, 643444.
533 18. Alfred, V., and Vaccari, T. (2016). When membranes need an ESCRT: endosomal sorting and
534 membrane remodelling in health and disease. Swiss Med Wkly *146*, w14347.

535 19. Radulovic, M., Schink, K.O., Wenzel, E.M., Nahse, V., Bongiovanni, A., Lafont, F., and Stenmark,
536 H. (2018). ESCRT-mediated lysosome repair precedes lysophagy and promotes cell survival.
537 EMBO J *37*.
538 20. Rodrigues, D., VijayRaghavan, K., Waltzer, L., and Inamdar, M.S. (2021). Intact in situ
539 Preparation of the Drosophila melanogaster Lymph Gland for a Comprehensive Analysis of
540 Larval Hematopoiesis. Bio-protocol *11*, e4204.
541 21. Duvic, B., Hoffmann, J.A., Meister, M., and Royet, J. (2002). Notch signaling controls lineage
542 specification during Drosophila larval hematopoiesis. Curr Biol *12*, 1923-1927.
543 22. Lebestky, T., Jung, S.H., and Banerjee, U. (2003). A Serrate-expressing signaling center controls
544 Drosophila hematopoiesis. Genes Dev *17*, 348-353.
545 23. Vaccari, T., and Bilder, D. (2005). The Drosophila tumor suppressor vps25 prevents
546 nonautonomous overproliferation by regulating notch trafficking. Dev Cell *9*, 687-698.
547 24. Palmer, W.H., and Deng, W.M. (2015). Ligand-Independent Mechanisms of Notch Activity.
548 Trends Cell Biol *25*, 697-707.
549 25. Morin-Poulard, I., Vincent, A., and Crozatier, M. (2013). The Drosophila JAK-STAT pathway in
550 blood cell formation and immunity. JAKSTAT *2*, e25700.
551 26. Herz, H.M., Chen, Z., Scherr, H., Lackey, M., Bolduc, C., and Bergmann, A. (2006). vps25
552 mosaics display non-autonomous cell survival and overgrowth, and autonomous apoptosis.
553 Development *133*, 1871-1880.
554 27. Khadilkar, R.J., Rodrigues, D., Mote, R.D., Sinha, A.R., Kulkarni, V., Magadi, S.S., and Inamdar,
555 M.S. (2014). ARF1-GTP regulates Asrij to provide endocytic control of Drosophila blood cell
556 homeostasis. Proc Natl Acad Sci U S A *111*, 4898-4903.
557 28. Pashkova, N., Gakhar, L., Winistorfer, S.C., Sunshine, A.B., Rich, M., Dunham, M.J., Yu, L., and
558 Piper, R.C. (2013). The yeast Alix homolog Bro1 functions as a ubiquitin receptor for protein
559 sorting into multivesicular endosomes. Dev Cell *25*, 520-533.
560 29. Bissig, C., and Gruenberg, J. (2014). ALIX and the multivesicular endosome: ALIX in
561 Wonderland. Trends Cell Biol *24*, 19-25.
562 30. Tabernero, L., and Woodman, P. (2018). Dissecting the role of His domain protein tyrosine
563 phosphatase/PTPN23 and ESCRTs in sorting activated epidermal growth factor receptor to the
564 multivesicular body. Biochem Soc Trans *46*, 1037-1046.
565 31. Tsunematsu, T., Yamauchi, E., Shibata, H., Maki, M., Ohta, T., and Konishi, H. (2010). Distinct
566 functions of human MVB12A and MVB12B in the ESCRT-I dependent on their posttranslational
567 modifications. Biochem Biophys Res Commun *399*, 232-237.
568 32. Matsuno, K., Diederich, R.J., Go, M.J., Blaumueller, C.M., and Artavanis-Tsakonas, S. (1995).
569 Deltex acts as a positive regulator of Notch signaling through interactions with the Notch
570 ankyrin repeats. Development *121*, 2633-2644.
571 33. Moretti, J., Chastagner, P., Gastaldello, S., Heuss, S.F., Dirac, A.M., Bernards, R., Masucci, M.G.,
572 Israel, A., and Brou, C. (2010). The translation initiation factor 3f (eIF3f) exhibits a
573 deubiquitinase activity regulating Notch activation. PLoS Biol *8*, e1000545.
574 34. Hori, K., Sen, A., Kirchhausen, T., and Artavanis-Tsakonas, S. (2012). Regulation of ligand-
575 independent Notch signal through intracellular trafficking. Commun Integr Biol *5*, 374-376.

576

577

578

579

580

581 **Figures**

582 **Figure 1. ESCRT components regulate ubiquitinated cargo sorting in the lymph gland.**

583 **(A)** Whole-mount larval lymph gland showing accumulation of conjugated ubiquitin (FK2) in the lymph
584 gland upon progenitor-specific (*domeGal4 UAS 2xEGFP* driven) knockdown of 7 *Drosophila* ESCRT
585 components indicated (Vps28, Tsg101, Vps37A, Vps22, Vps32, Vps20, Vps2). Ubiquitin staining is
586 shown in gray scale. Accumulation of ubiquitin aggregates is marked by arrowhead and magnified in
587 insets. Scale bar: 100 µm. **(B)** Bar diagrams show quantification of the fraction of cells accumulating
588 ubiquitin aggregates in primary, secondary and tertiary lobes upon knockdown of all 13 core ESCRT
589 components. n indicates the number of individual lobes analysed and N indicates the number of larvae
590 analysed. Error bars represent SEM. Kruskal Wallis test was performed to determine the statistical
591 significance. *P<0.05, P**<0.01, ***P<0.001. Summary chart indicating presence (colored box) or
592 absence (white box) of ubiquitin accumulation in the primary, secondary and tertiary lobes upon
593 depletion of the respective ESCRT component (left).

594

595 **Figure 2. ESCRT components regulate progenitor maintenance and plasmatocyte differentiation in**
596 **the lymph gland.**

597 **(A)** Whole-mount larval lymph gland showing change in the fraction of dome>2xEGFP+ve progenitors
598 (green) or P1+ve plasmatocytes (red) in the lymph gland upon progenitor-specific knockdown of 6
599 ESCRT components (Hrs, Vps28, Vps37A, Vps36, Vps32, Vps2). Scale bar: 100 µm. **(B-C)** Bar diagrams
600 shows quantification of the fraction of progenitors (B) and plasmatocytes (C) in primary, secondary
601 and tertiary lobes upon knockdown of all 13 core ESCRT components. n indicates the number of
602 individual lobes analysed and N indicates the number of larvae analysed. Error bars represent SEM.
603 Kruskal Wallis test was performed to determine the statistical significance. *P<0.05, **P<0.01,
604 ***P<0.001. Summary chart indicating presence (colored box) or absence (white box) of phenotypes
605 of progenitor loss (B) or increased plasmatocytes differentiation (C) in the primary, secondary and
606 tertiary lobes upon depletion of the respective ESCRT component (left). Also see Fig. 6, Fig.S1.

607

608 **Figure 3. ESCRT components differentially regulate crystal cell differentiation of lymph gland**
609 **progenitors.**

610 **(A)** Whole-mount larval lymph gland showing increase in differentiation of ProPO+ve crystal cells (red)
611 in the lymph gland upon progenitor-specific knockdown of 12 core ESCRT components (All except
612 Vps25). Dome>2xEGFP (green) marks the progenitors across different lobes. Arrowheads mark

613 presence of crystal cells in posterior lobes. Scale bar: 100 µm. **(B)** Bar diagram shows quantification of
614 the fraction of crystal cells in primary, secondary and tertiary lobes upon knockdown of all 13 core
615 ESCRT components. n indicates the number of individual lobes analysed and N indicates the number
616 of larvae analysed. Error bars represent SEM. Kruskal Wallis test was performed to determine the
617 statistical significance. *P<0.05, **P<0.01, ***P<0.001. Summary chart indicating presence (colored
618 box) or absence (white box) of phenotypes of increased crystal cell differentiation in the primary,
619 secondary and tertiary lobes upon depletion of the respective ESCRT component (left). Also see Fig.
620 6.

621

622 **Figure 4. ESCRT components regulate Notch activation and NICD trafficking in the lymph gland.**

623 **(A)** Whole-mount larval lymph gland showing NRE-GFP+ve (Notch reporter) cells (green) and dome+ve
624 progenitors (red) in primary lobes upon progenitor-specific knockdown of 8 representative ESCRT
625 components indicated [Hrs, Stam (ESCRT-0); Vps28, Tsg101 (ESCRT-I); Vps25, Vps22 (ESCRT-II); Vps32,
626 Vps24 (ESCRT-III)]. Scale bar: 100 µm. Bar diagrams show quantification of the number of NRE-GFP
627 positive cells in primary, secondary and tertiary lobes upon knockdown of the same 8 ESCRT
628 components. **(B)** Whole-mount larval lymph gland showing NICD expression (shown in red in the upper
629 panel and in gray scale in the lower panel) in primary lobes upon progenitor-specific knockdown of
630 the same 8 aforementioned ESCRT components. Progenitors are marked by dome>2xEGFP (green).
631 Scale bar: 100 µm. (B') Magnified view showing lymph gland hemocytes with (arrow) or without
632 (arrowhead) NICD accumulation. Scale bar: 10 µm. Bar diagrams show quantification of the number
633 of NICD accumulating cells in primary, secondary and tertiary lobes. n indicates the number of
634 individual lobes analysed and N indicates the number of larvae analysed. Error bars represent SEM.
635 One-way ANOVA was performed to determine the statistical significance. *P<0.05, **P<0.01,
636 ***P<0.001. See also Fig S4.

637

638 **Figure 5. ESCRT components regulate lamellocyte differentiation in the lymph gland.**

639 **(A)** Whole-mount larval lymph gland showing Phalloidin staining (red) to visualise elongated
640 morphology of lamellocytes upon progenitor-specific knockdown of 5 ESCRT components (Tsg101,
641 Vps37A, Vps36, Vps20, Vps2). Blue arrowheads mark the region from primary, secondary or tertiary
642 lobes, magnified in the insets. The inset panel shows enlarged view of Phalloidin staining with
643 lamellocytes marked by orange arrowhead. Scale bar: 100 µm. **(B)** Bar diagram shows quantification
644 of the percentage of lymph glands showing lamellocyte differentiation in primary, secondary and

645 tertiary lobes upon knockdown of all 13 core ESCRT components, without any immune challenge.
646 Values in the columns indicate the number of larvae analysed for presence or absence of lamellocytes.
647 Summary chart indicating presence (colored box) or absence (white box) of lamellocytes
648 differentiation in the primary, secondary and tertiary lobes upon depletion of the respective ESCRT
649 component (left). **(C)** Whole-mount lymph glands of Vps25 KD (*domeGal4 UAS 2xEGFP; UAS Vps25*
650 *RNAi;+/+*) and Vps32 KD (*domeGal4 UAS 2xEGFP; UAS Vps32 RNAi;+/+*) larvae uninfested or 3 days
651 after wasp infestation. Phalloidin staining shows presence of lamellocytes (marked by orange
652 arrowhead in the inset). Schematic representing the phenotype of Vps25 KD and Vps32 KD lymph
653 glands with and without wasp infestation. Box marks lamellocyte differentiation in posterior lobes.
654 See also, Fig 6.

655

656 **Figure 6. A spatiotemporal map indicating ESCRT function in cargo sorting, progenitor maintenance**
657 **and lineage-specific differentiation in *Drosophila* larval hematopoiesis.**

658 **(A)** Schematic representation of lymph gland lobes from anterior to posterior (left to right). Green
659 circle (medullary zone) in primary lobe and green dotted lines in posterior lobe indicates the
660 progenitor pool depleted of ESCRT components (13 genes from ESCRT-0, I, II and III). Blood cell types
661 are represented as violet (plasmatocytes), pink (crystal cells) and blue (lamellocytes). Red font denotes
662 ESCRT components whose depletion affected a given lineage whereas grey font indicates that there
663 was no discernible change. Red monochrome heatmap indicates position-dependent progenitor
664 sensitivity to depletion of ESCRT. See also Fig S2. **(B)** Comprehensive summary chart of the effects of
665 individual ESCRT depletion on the various aspects of hematopoiesis as indicated. Presence or absence
666 of a phenotype is depicted by colored or white boxes respectively. Red asterisk indicates Notch
667 pathway activation and grey asterisk indicates no change, for components that were tested. **(C)** Venn
668 diagram showing superimposition of phenotypes caused by the knockdown of different ESCRT
669 components from progenitors. The underlined components in the lower panel affect both ubiquitin
670 accumulation and progenitor status as described in the upper panel and (B).

671

672 **Figure 7. ESCRT cell-autonomously regulates ubiquitinated cargo sorting in the lymph gland**
673 **progenitors but may regulate differentiation in non-autonomous manner as well.**

674 **(A)** Whole-mount lymph glands showing immunostaining for conjugated ubiquitin (red) in control
675 (*domeGal4/+; neoFRT42D/+; UAS mCD8 RFP/+*) and progenitor-specific mutant clone of
676 representative ESCRT component Vps32/shrub (*domeGal4/+; shrb^{G5} neoFRT42D/neoFRT42D; UAS*

677 *mCD8 RFP/UAS FLP*). Area marked by blue arrowheads are magnified in the insets to show
678 homozygous mitotic clones (GFP-ve patch, demarcated by dotted white line). Orange arrowheads
679 indicate ubiquitin accumulation in the mutant cells. DAPI marks the nuclei. **(B)** Primary lobe of control
680 and Vps32 mutant clone showing ProPO staining (red) to mark crystal cells. Arrowheads mark the
681 crystal cells which are GFP-ve (homozygous mutant). **(C)** Phalloidin staining in the same genotypes
682 shows GFP+ elongated and coalescing cells marked by arrowheads (insets) in the mutant clone. Scale
683 bar in all image panels: 100 µm.

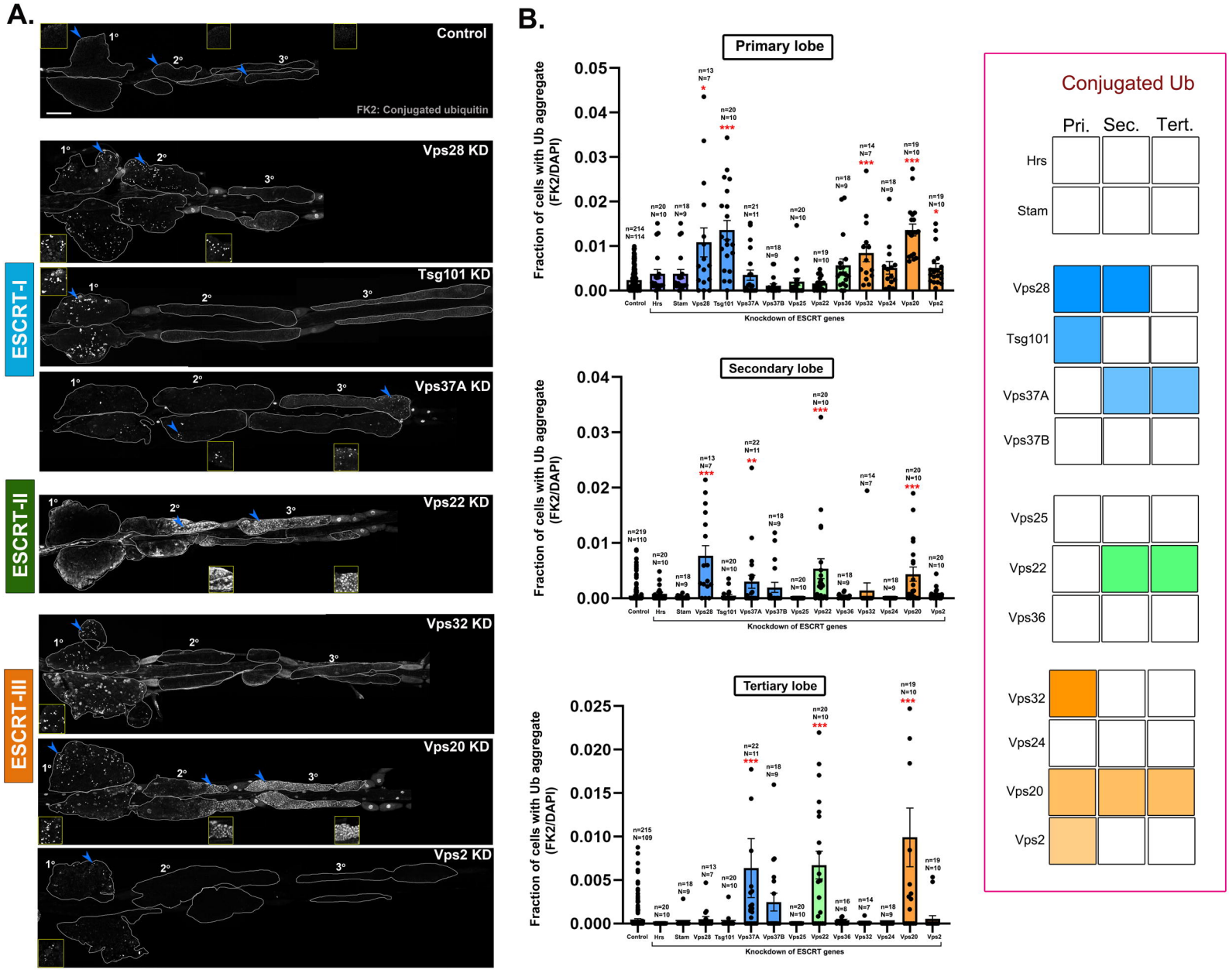
A.
Control
FK2: Conjugated ubiquitin
Vps28 KD
Tsg101 KD
Vps37A KD
Vps22 KD
Vps32 KD
Vps20 KD
Vps2 KD
ESCRT-I
ESCRT-II
ESCRT-III
1°
2°
3°
B.
Primary lobe
Secondary lobe
Tertiary lobe
Fraction of cells with Ub aggregate (FK2/DAPI)
Knockdown of ESCRT genes
Control
Hrs
Stam
Vps28
Tsg101
Vps37A
Vps37B
Vps25
Vps22
Vps36
Vps32
Vps24
Vps20
Vps2
Conjugated Ub
Pri.
Sec.
Tert.

Figure 1

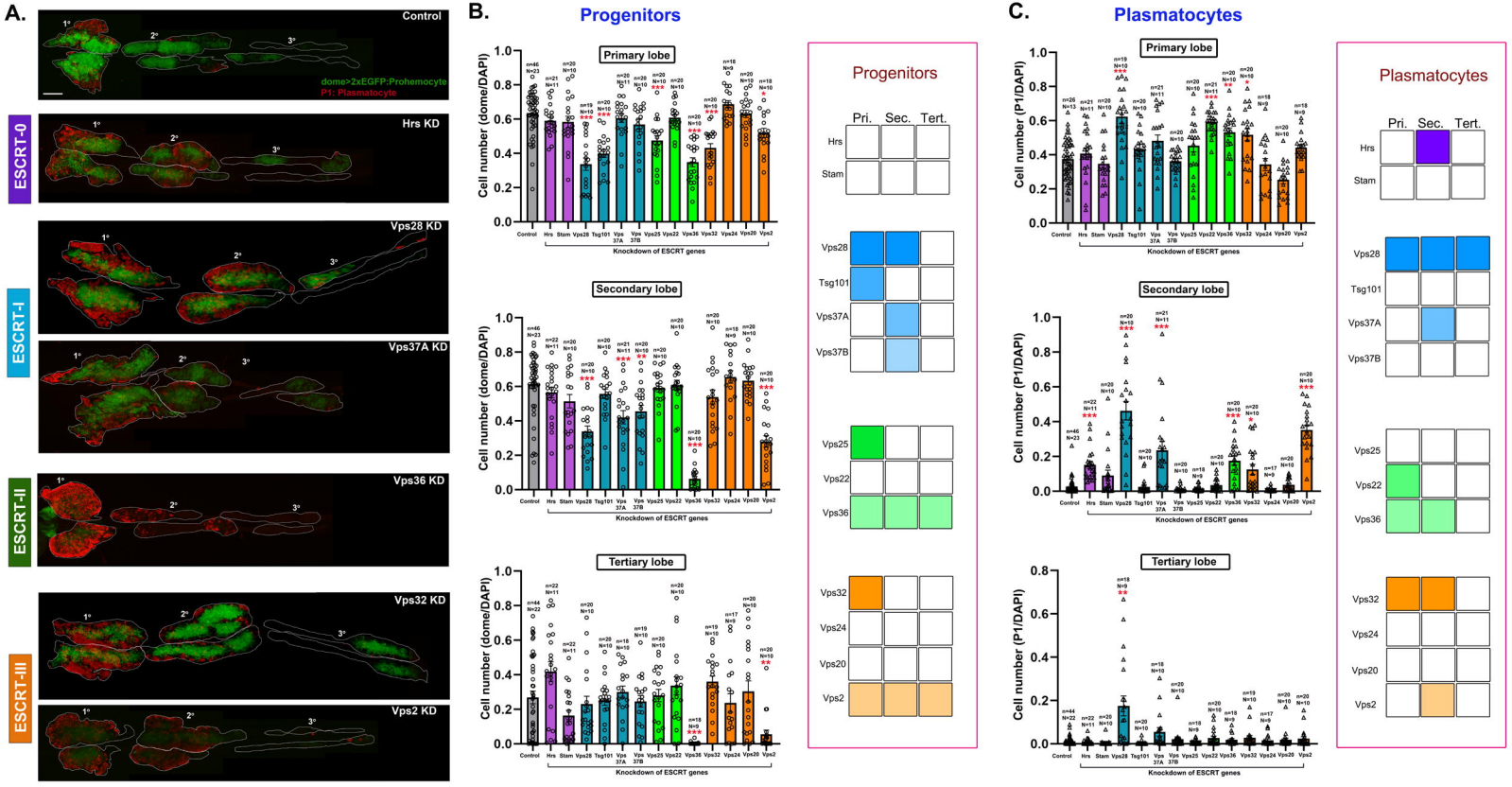
A.
Control
dome>2xEGFP:Prohemocyte
P1: Plasmatocyte
ESCRT-0
Hrs KD
ESCRT-I
Vps28 KD
Vps37A KD
ESCRT-II
Vps36 KD
ESCRT-III
Vps32 KD
Vps2 KD
B.
Progenitors
Primary lobe
Secondary lobe
Tertiary lobe
Cell number (dome/DAPI)
Knockdown of ESCRT genes
Control
Hrs
Stam
Vps28
Tsg101
Vps 37A
Vps 37B
Vps25
Vps22
Vps36
Vps32
Vps24
Vps20
Vps2
Progenitors
Pri.
Sec.
Tert.
C.
Plasmatocytes
Primary lobe
Secondary lobe
Tertiary lobe
Cell number (P1/DAPI)
Knockdown of ESCRT genes
Plasmatocytes

Figure 2

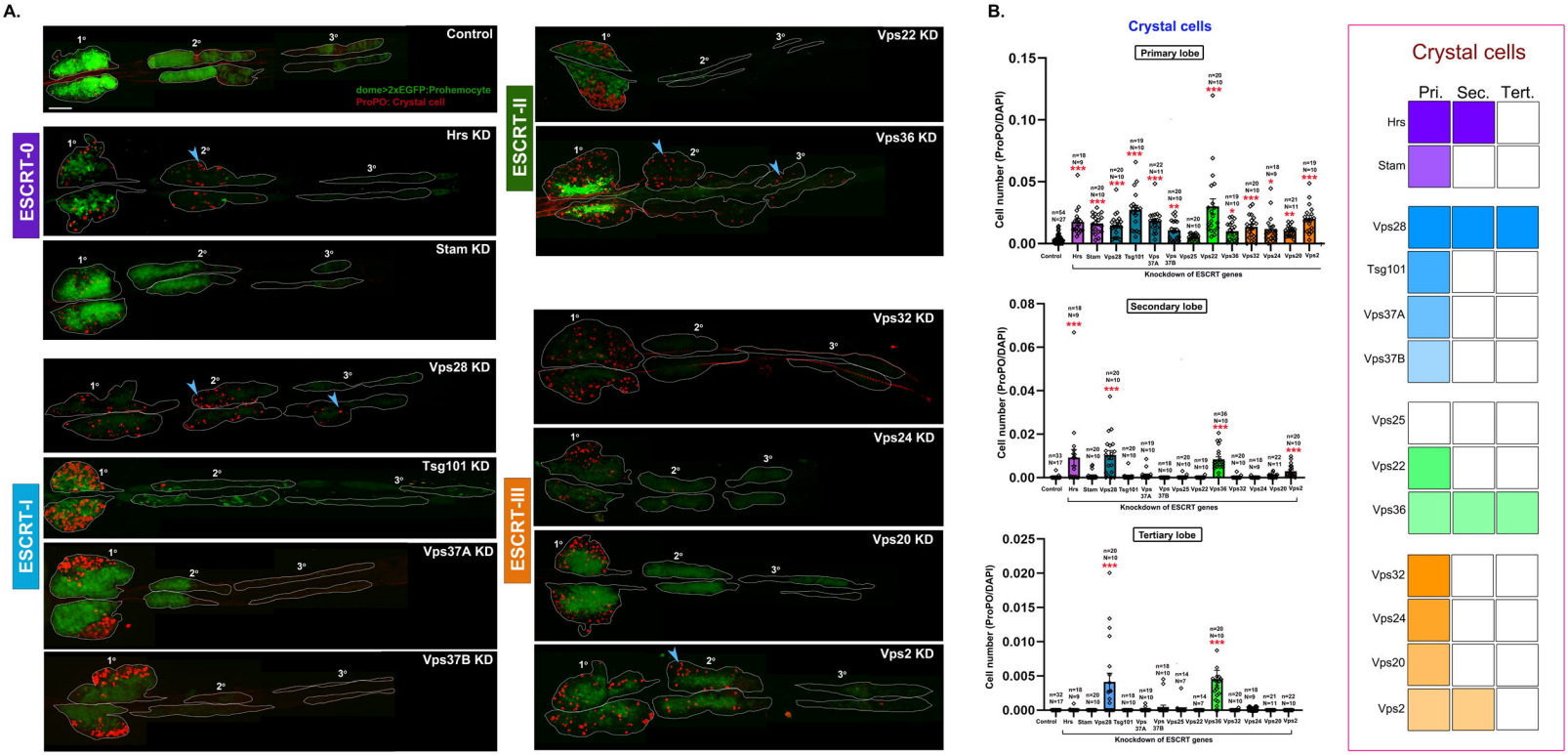
A.
Control
dome>2xEGFP:Prohemocyte
ProPO: Crystal cell
ESCRT-0
Hrs KD
Stam KD
ESCRT-I
Vps28 KD
Tsg101 KD
Vps37A KD
Vps37B KD
ESCRT-II
Vps22 KD
Vps36 KD
ESCRT-III
Vps32 KD
Vps24 KD
Vps20 KD
Vps2 KD
1°
2°
3°
B.
Crystal cells
Primary lobe
Secondary lobe
Tertiary lobe
Cell number (ProPO/DAPI)
Knockdown of ESCRT genes
Control
Hrs
Stam
Vps28
Tsg101
Vps 37A
Vps 37B
Vps25
Vps22
Vps36
Vps32
Vps24
Vps20
Vps2
Crystal cells
Pri.
Sec.
Tert.
Hrs
Stam
Vps28
Tsg101
Vps37A
Vps37B
Vps25
Vps22
Vps36
Vps32
Vps24
Vps20
Vps2

Figure 3

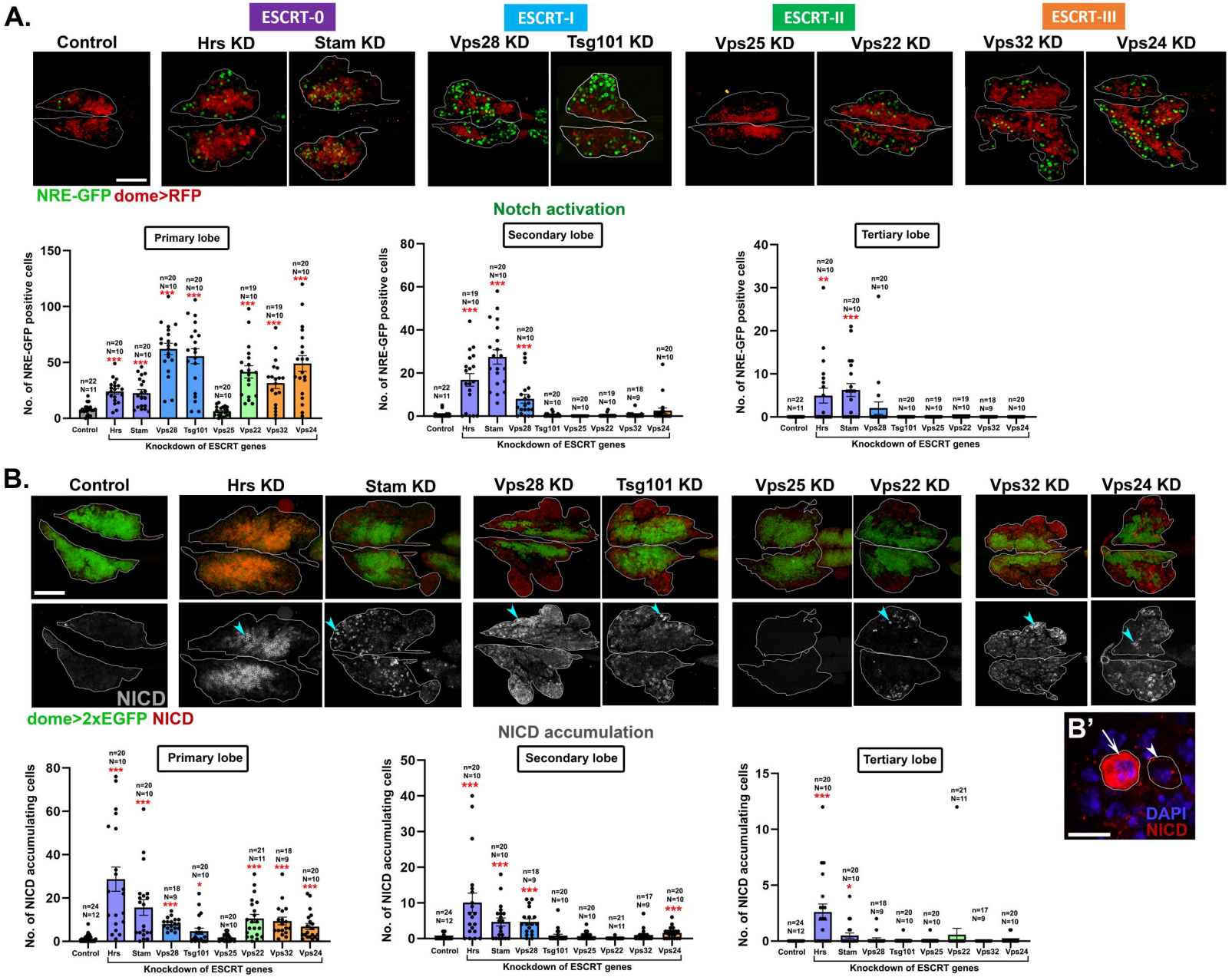
A.
ESCRT-0
ESCRT-I
ESCRT-II
ESCRT-III
Control
Hrs KD
Stam KD
Vps28 KD
Tsg101 KD
Vps25 KD
Vps22 KD
Vps32 KD
Vps24 KD
NRE-GFP dome>RFP
Notch activation
Primary lobe
Secondary lobe
Tertiary lobe
No. of NRE-GFP positive cells
Knockdown of ESCRT genes
B.
NICD
dome>2xEGFP NICD
NICD accumulation
No. of NICD accumulating cells
B'
DAPI
NICD

Figure 4

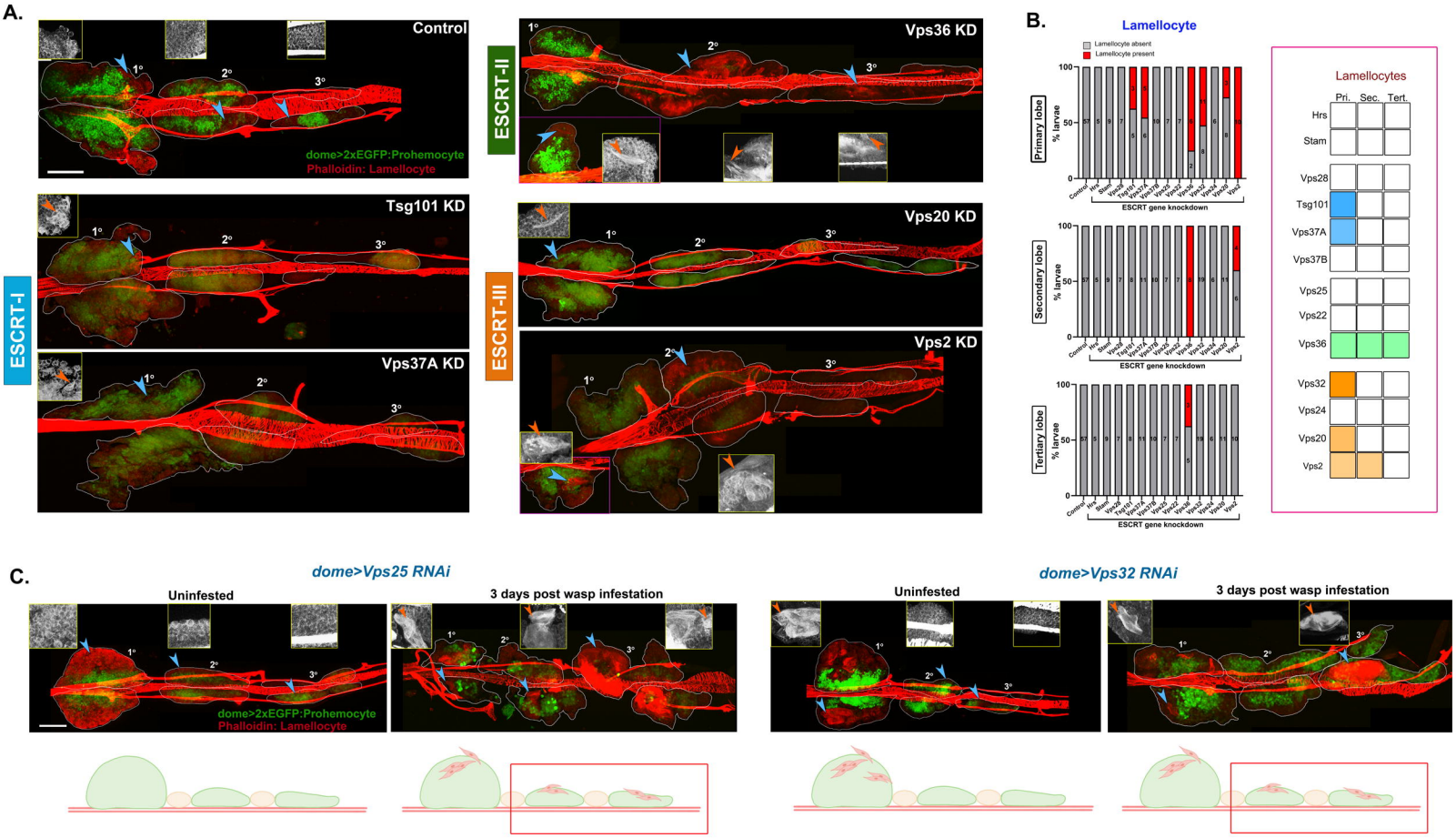
A.
Control
dome>2xEGFP:Prohemocyte
Phalloidin: Lamellocyte
ESCRT-I
Tsg101 KD
Vps37A KD
ESCRT-II
Vps36 KD
ESCRT-III
Vps20 KD
Vps2 KD
B.
Lamellocyte
Lamellocyte absent
Lamellocyte present
Primary lobe
Secondary lobe
Tertiary lobe
% larvae
ESCRT gene knockdown
Lamellocytes
Pri.
Sec.
Tert.
Hrs
Stam
Vps28
Tsg101
Vps37A
Vps37B
Vps25
Vps22
Vps36
Vps32
Vps24
Vps20
Vps2
C.
dome>Vps25 RNAi
Uninfested
3 days post wasp infestation
dome>2xEGFP:Prohemocyte
Phalloidin: Lamellocyte
dome>Vps32 RNAi
Uninfested
3 days post wasp infestation

Figure 5

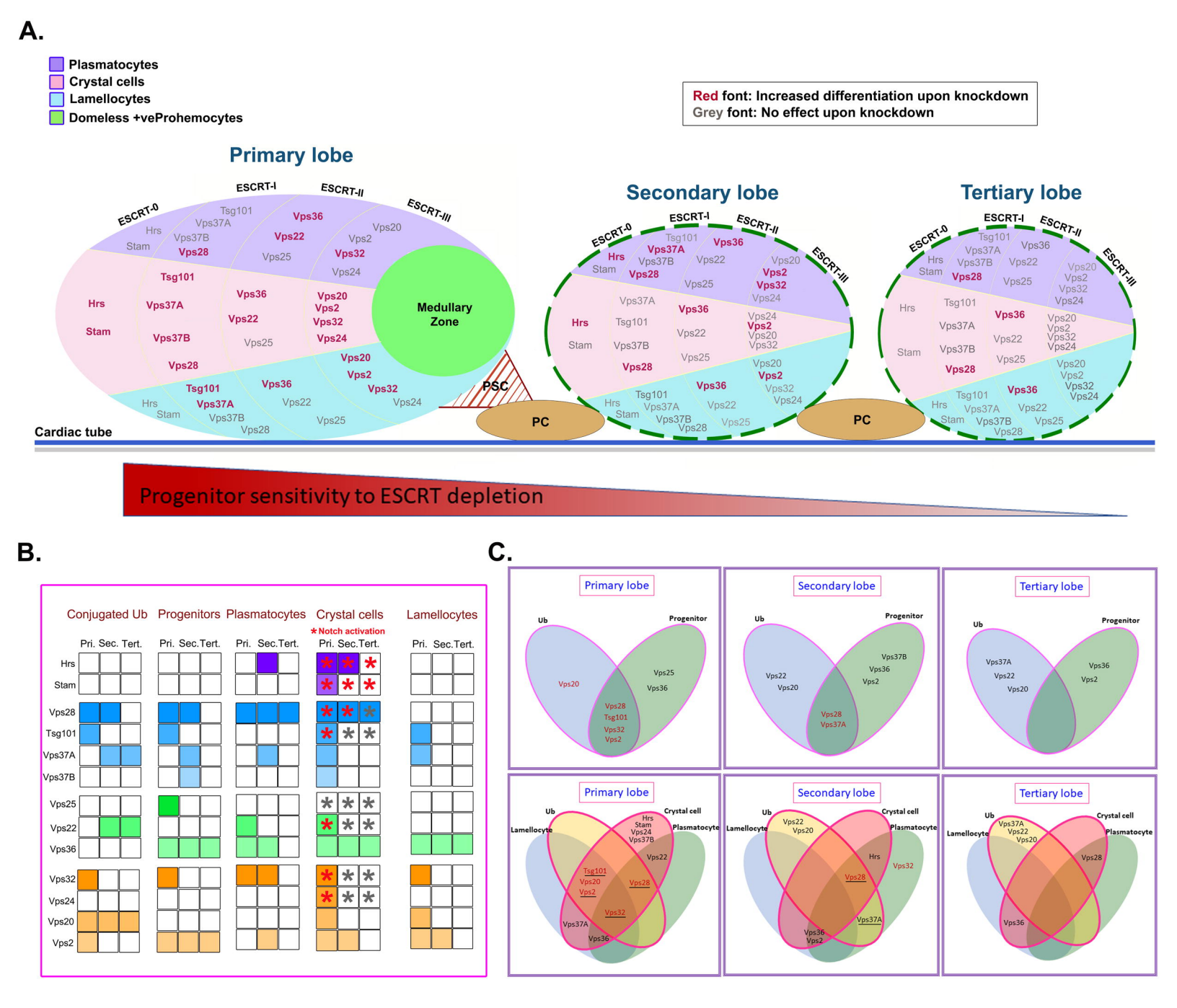
A.
Plasmatocytes
Crystal cells
Lamellocytes
Domeless +veProhemocytes
Red font: Increased differentiation upon knockdown
Grey font: No effect upon knockdown
Primary lobe
Secondary lobe
Tertiary lobe
ESCRT-0
ESCRT-I
ESCRT-II
ESCRT-III
Medullary Zone
PSC
PC
Cardiac tube
Progenitor sensitivity to ESCRT depletion
B.
Conjugated Ub
Progenitors
Plasmatocytes
Crystal cells
Lamellocytes
Notch activation
Pri. Sec. Tert.
Hrs
Stam
Vps28
Tsg101
Vps37A
Vps37B
Vps25
Vps22
Vps36
Vps32
Vps24
Vps20
Vps2
C.
Primary lobe
Secondary lobe
Tertiary lobe
Ub
Progenitor
Crystal cell
Lamellocyte
Plasmatocyte

Figure 6

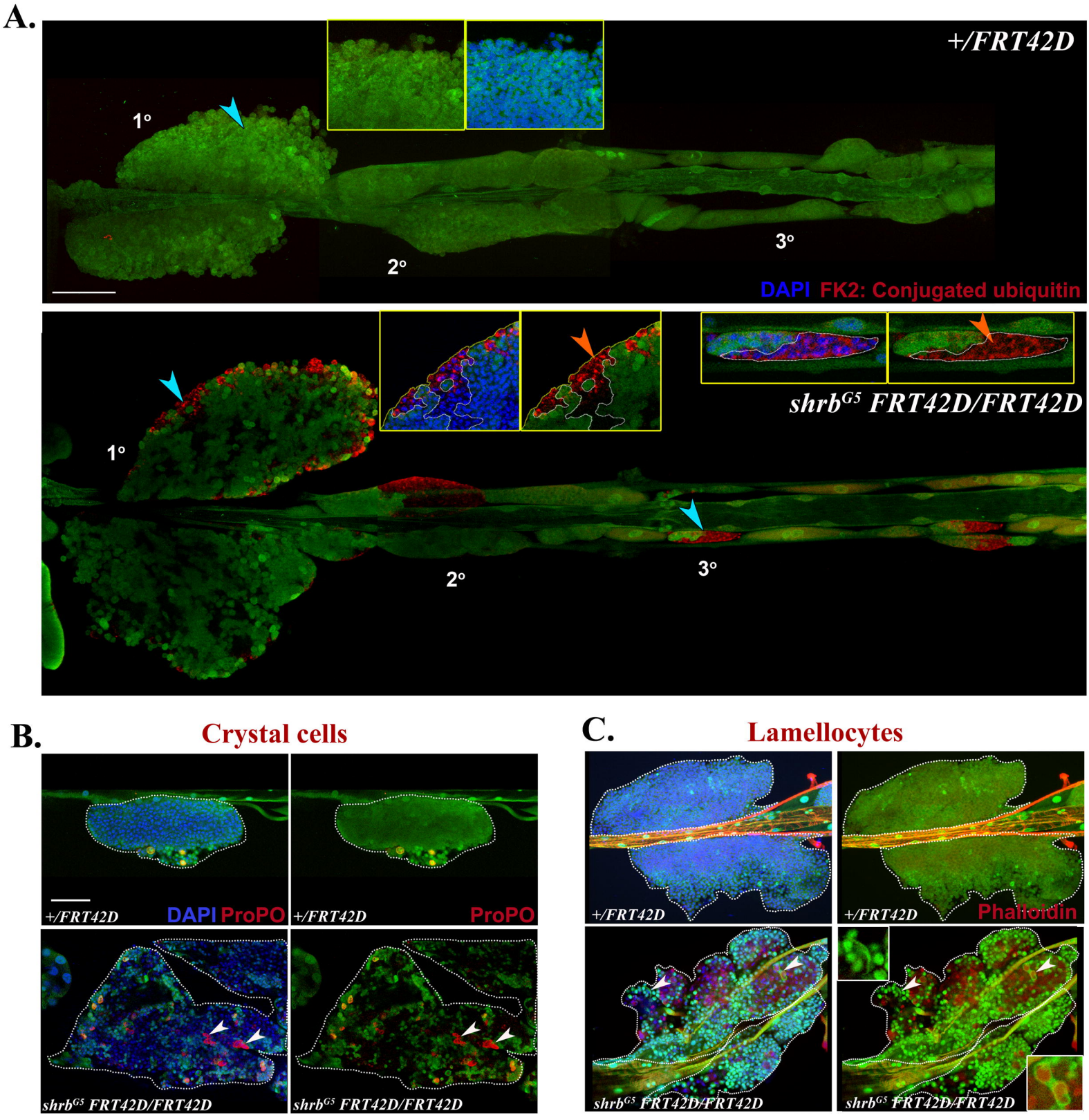
A.
+/FRT42D
1°
2°
3°
DAPI FK2: Conjugated ubiquitin
shrb^{G5} FRT42D/FRT42D
1°
2°
3°
B.
Crystal cells
+/FRT42D
DAPI ProPO
+/FRT42D
ProPO
shrb^{G5} FRT42D/FRT42D
shrb^{G5} FRT42D/FRT42D
C.
Lamellocytes
+/FRT42D
+/FRT42D
Phalloidin
shrb^{G5} FRT42D/FRT42D
shrb^{G5} FRT42D/FRT42D

Figure 7